

# Seismic Design of Lightly Reinforced Precast Concrete Rectangular Wall Panels

## Francisco J. Crisafulli, Ph.D.

Professor  
Facultad de Ingeniería  
Universidad Nacional de Cuyo  
Mendoza, Argentina



## José I. Restrepo, Ph.D.

Associate Professor  
Department of Structural Engineering  
University of California, San Diego  
La Jolla, California



## Robert Park, Ph.D.

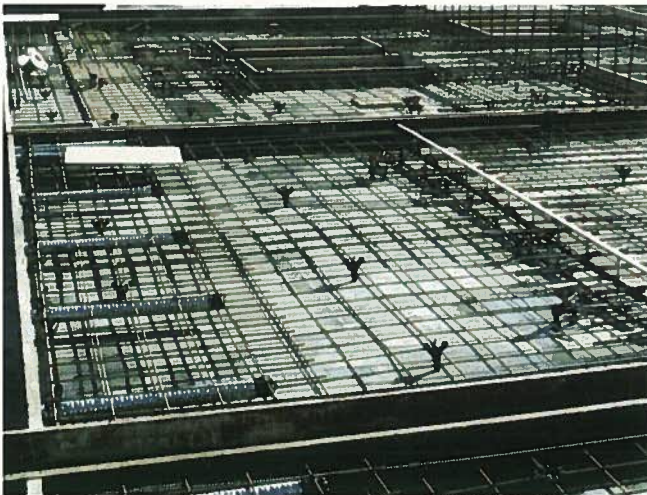
Emeritus Professor  
Department of Civil Engineering  
University of Canterbury  
Christchurch, New Zealand

---

*Lightly reinforced precast concrete panels can be used advantageously to provide lateral force resistance in low-rise buildings. The abundance of wall panels in certain buildings means that wall panels that are lightly reinforced can provide sufficient lateral force resistance if designed for nominally elastic or limited ductility response. In these systems, the ductility demand in the critical regions of the walls is expected to be low and, as a result, the detailing of the critical regions can be eased without having any detrimental effect on the overall seismic performance. This paper presents theoretical and practical aspects relevant to the seismic design and behavior of precast concrete rectangular walls that are jointed at the foundation. Particular emphasis is given to the stiffness, useable lateral displacement ductility and the shear transfer in the connection. Experimental results of a test on a single wall unit are also discussed in the paper. A numerical design example is included to show the application of the proposed system.*

---

**S**ince the early 1960s, there has been a worldwide increase in the use of precast concrete for structural components in buildings. This has come about because the incorporation of precast concrete components has the advantages of high quality control, reduction of site formwork and labor, increased speed of construction, and overall economy.



(a) Reinforcing cage and ducting



(b) Wall panel before erection



(c) Protruding bars used in wall panel connection



(d) Erection of panel

Fig. 1. Example of precast concrete walls connected through grouted ducting.

In some seismic regions, the extensive use of precast components has been limited because of the poor earthquake performance of reinforced concrete structures incorporating precast concrete elements. This situation has been aggravated by the fact that building codes in many countries have, for many years, contained comprehensive provisions for the seismic design of cast-in-place concrete structures but not for the design of precast concrete structures.

Precast concrete walls that cantilever from the foundation can be used in the construction of low-rise commercial and industrial buildings as part of the lateral force resisting system. Once erected, the wall panels are connected

to the adjacent structural elements, such as slabs and foundations, with jointed connections comprising various combinations of concrete inserts, bolted or welded steel plates or angle brackets, lapped reinforcement splices within cast-in-place joining strips, and grouted bars in sleeves or ducts.<sup>1,2</sup>

A precast concrete system that is commonly used in New Zealand uses the connection shown in Figs. 1 and 2. In this system, the vertical bars protruding from the foundation are grouted into galvanized corrugated steel ducts embedded in the wall units a distance at least equal to the development length.

The ducts are purposely made larger to ease the erection of the walls. They

have an inside diameter that is typically equal to the diameter of the bar to be anchored plus a void of 1 to 2 in. (25 to 50 mm). The ducts and the wall-foundation gap are grouted in a single operation or, alternatively, the gap is dry-packed and then the ducts are grouted.

Shrinkage-compensating cement-based grouts, which are either pumped or poured from the wall-foundation gap, are normally used. The grout is pumped in to ensure it flows in one direction to avoid the entrapment of air. Air is expelled through vents placed at several locations on the gap as well as at the upper end of each duct. A minimum distance of at least 3 in. (75 mm) is normally left between the end of the



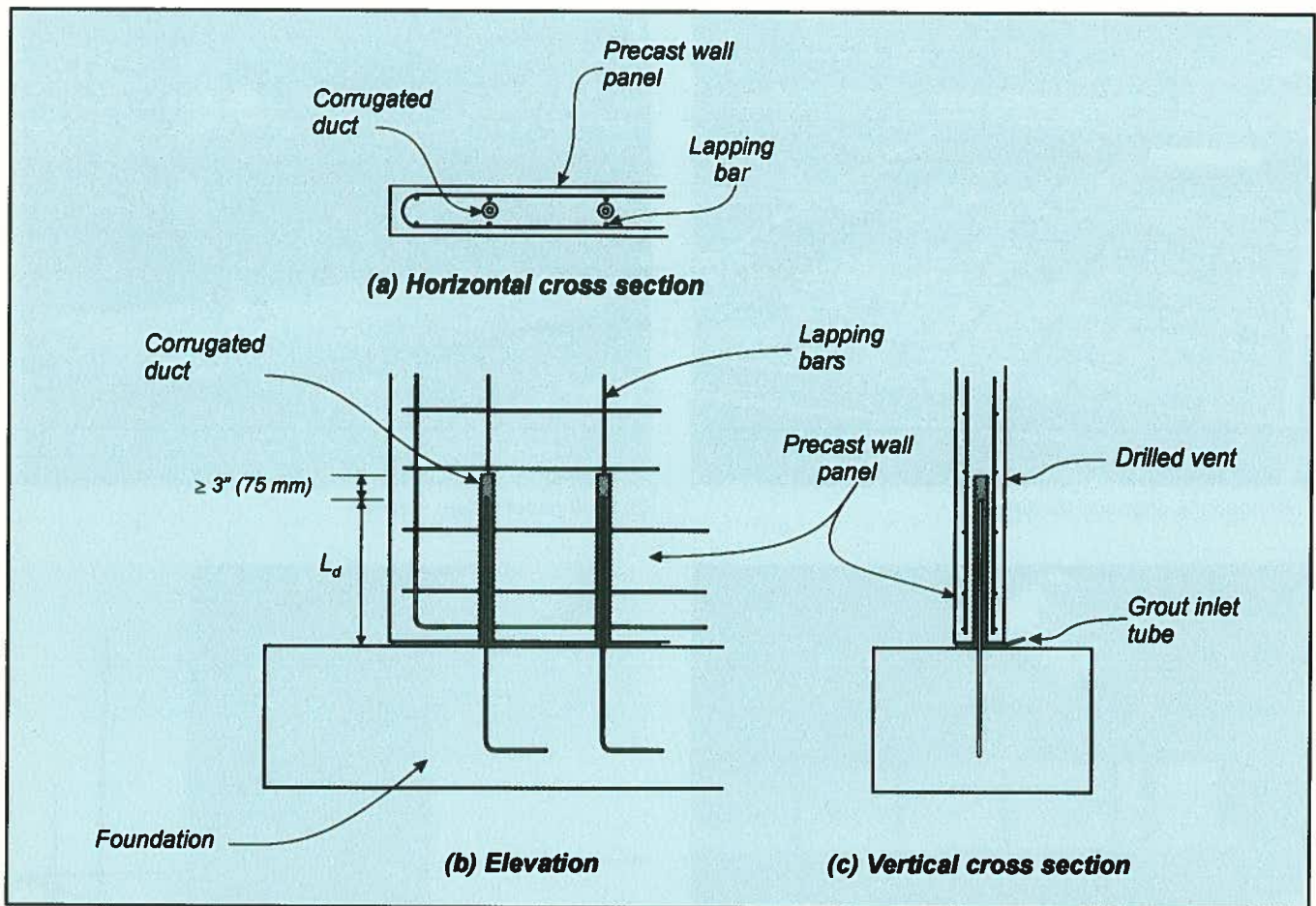


Fig. 2. Wall panel-to-foundation connection detail.

vertical bar and the end of the duct.

This distance is in recognition that water bleeding in the upper end of the duct can lower the mechanical properties of the grout. Prior to grouting, the base of the wall and the foundation beam are roughened and cleaned with an oil-free air pressure gun to improve the interface shear transfer conditions. The force transfer between the wall panel and the foundation is achieved through non-contact lap bar splices from the grouted bars and bars that are cast with the wall unit.

Frequently, during the seismic design of low-rise buildings in which the lateral force resistance is provided by structural walls, it can be found that, when following the recommendations for the design of cast-in-place concrete walls, minimum provisions control the amount of longitudinal wall reinforcement and the detailing of the transverse reinforcement at the potential plastic hinge regions. It can also be found that minimum design provisions would also control the design of the walls

even if the lateral forces considered were derived from an elastic response spectrum without being reduced by a response modification factor.

A building in which the walls are detailed with the minimum provisions, and where a rigorous capacity design procedure is not performed, might not necessarily be sufficiently strong and ductile. This is because the weak link could be hidden in a structural component or in a connection that is not specifically detailed for ductility.

Design provisions specifically written for cast-in-place concrete walls could be of questionable use when using some precast concrete wall systems. For example, the design provision for establishing the minimum amount of longitudinal reinforcement in cast-in-place concrete walls is to ensure a moment capacity greater than the cracking moment. Nonetheless, the use of such a criterion seems inappropriate for the type of precast system described above (see Fig. 2). Little, if any, tension can be transferred across

the connection and, thus, the bending moment is very small since it depends mainly on the axial force present in the wall.

Precast concrete walls of this type could be designed as "if jointed" with longitudinal reinforcement amounts that are less than the minimum recommended for cast-in place concrete wall construction. In such designs, the walls are expected to develop a single crack at the wall-foundation connection when subjected to in-plane lateral loading in a strong earthquake.

The potential disadvantages that could affect the overall seismic response of these walls are the very small plastic hinge length and the tendency for sliding shear to occur once the connection opens up. If such a system is to be recommended for use in practice, it must be demonstrated that these two potential disadvantages are explicitly addressed during the design process to ensure they have no influence on the system's overall seismic response.

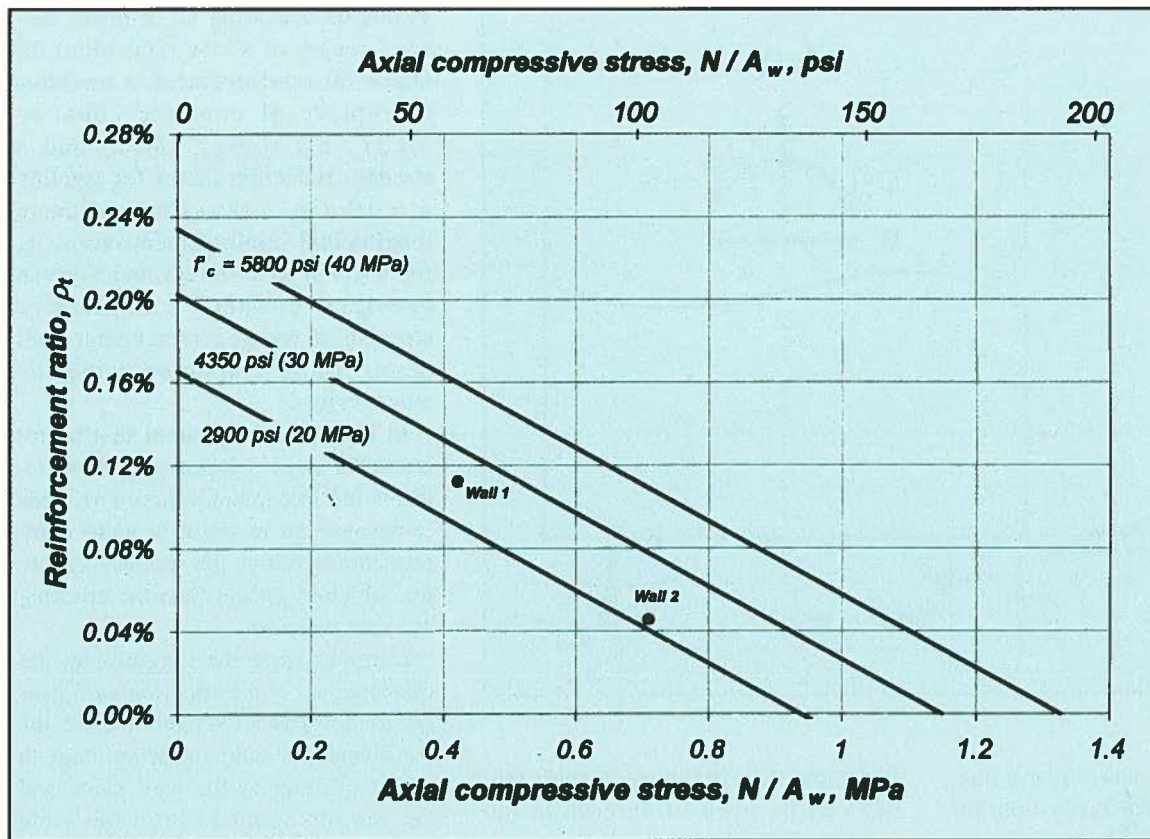


Fig. 3. Axial compression-longitudinal reinforcement ratio interaction diagram for inducing flexural cracking in rectangular walls.

This paper discusses the theoretical aspects required for the seismic design of lightly reinforced precast concrete walls that are jointed at the foundation and that are suitable for providing earthquake resistance in low-rise buildings. The article focuses on the design of cantilever wall panels that remain uncracked and whose nonlinear lateral force lateral displacement response is due to the opening of a gap at the wall-foundation connection. The paper also reviews the results obtained from a cyclic reversed loading test on a full-scale precast concrete wall unit. A numerical design example is provided to show the application of the proposed design system.

## LITERATURE REVIEW

A review of the literature indicates that there is limited knowledge about the seismic response of precast concrete wall systems and connections used in construction. In precast concrete wall construction, it is particularly difficult to develop systems that can truly emulate monolithic behavior.

This is because the connections at

the base of the walls often require the splicing of longitudinal reinforcement at the critical region where plastic hinges would normally be expected to occur. Splicing of the longitudinal reinforcement generally precludes the spread of the plastic hinge into the wall panel, thus, constraining the plasticity to develop only at the wall-foundation connection.

Monolithic emulation can be achieved in systems whose walls are embedded in a grouted recess in the foundation.<sup>3</sup> Most other systems rely on shear transfer across the connection, but little emphasis is given to the effect caused by the opening there. The design for shear transfer across the connection is often done following the shear-friction concepts proposed in the 1960s<sup>4,5</sup> and incorporated in the building codes.

Experimental work on the shear transfer across joints is fairly extensive, with numerous results available on tests on specimens tested monotonically under combined shear and axial load conditions. Experimental work investigating the effects the cyclic loading has on the shear transfer mechanisms is more limited.<sup>6,7</sup>

The present work has been carried out on specimens subjected to reversed cyclic shear and constant axial force, but without overturning moment. This loading condition is useful as it identifies the main components of the shear transfer mechanisms. However, the boundary conditions of these tests do not represent very well the conditions of wall panels subjected to seismic actions, particularly when the reversed cyclic bending moments exceeding the yield rotation are applied at the connection.

## THEORETICAL CONSIDERATIONS

Presented herein are general design criteria, design for combined flexure-axial load and shear, and overall lateral force-lateral displacement response.

### General Design Criteria

The precast concrete walls described in this paper are suitable for furnishing satisfactory in-plane lateral force resistance if the principles of capacity design are used to preclude any undesir-



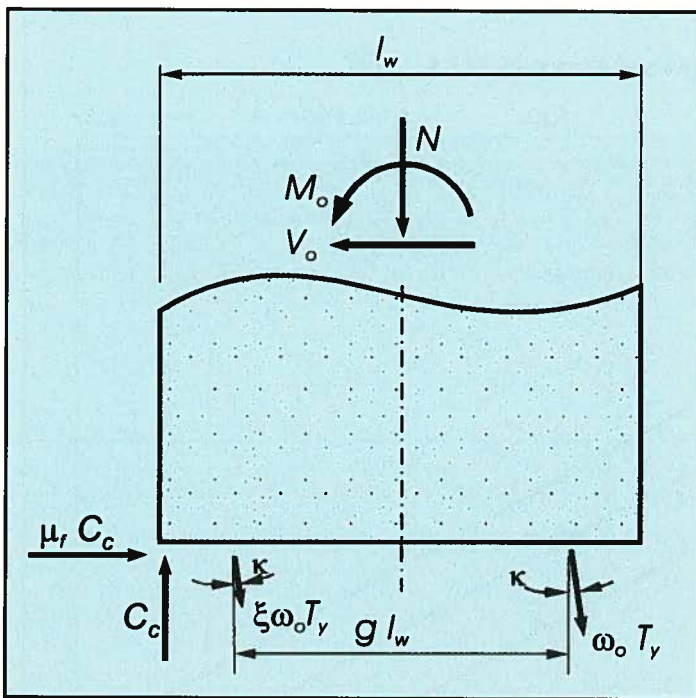


Fig. 4. Shear resisting mechanisms at joint between a wall panel and foundation.

able mode of failure, ensuring that non-linear behavior results chiefly from the opening of the wall-foundation connection. When detailing the wall panels with longitudinal reinforcing steel ratios less than those required to resist the cracking moment of the wall section, the wall panels should be designed to remain uncracked during erection and all other loading conditions.

This behavior is desirable because of (a) serviceability requirements, and (b) potential structural problems associated with the brittle flexural post-cracking behavior of the panels. In terms of capacity design, the latter condition implies that the walls should be able to develop the flexural over-strength while preventing cracking in the wall panel and preventing a sliding shear failure at the wall-foundation connection.

### Design for Combined Flexure-Axial Load

A main feature of this precast wall system is that tensile stresses cannot develop between the cementitious interfaces at the connection region, and, therefore, the building code requirements for minimum flexural reinforcement and reinforcement spacing, which may often control the design of a wall panel, do not have to be satis-

fied there. Conventional flexural theory can be used to determine the amount of longitudinal reinforcement required. Ductile reinforcement, preferably with a tensile strain at the ultimate tensile strength of at least 12 percent, is required to accommodate the relatively high strain demands that are expected to arise in the longitudinal bars crossing the wall-foundation connection in a strong earthquake.

Another feature of this precast concrete system is that the neutral axis depth-to-wall length ratios at the ultimate limit state are typically less than 0.08. Given the shallowness of the neutral axis depths, flexural failure in this system is often initiated by fracturing of the longitudinal reinforcement at the wall-foundation connection rather than by crushing of the compressed concrete.

If the reinforcement ratio of the longitudinal bars crossing the connection and that provided in the wall panel is less than that required by the building code for cast-in-place walls, the wall panel should be designed to remain uncracked at all stages of loading, including at the stage associated with the development of the flexural over-strength.

It is suggested here that, in place of a statistical sample, the flexural over-strength at the connection region be

evaluated assuming an ultimate tensile strength of 87 ksi (600 MPa) for Grade 60 reinforcement, a modulus of rupture of concrete equal to  $7.2\sqrt{f'_c}$  psi ( $0.6\sqrt{f'_c}$  MPa) and a strength reduction factor for bending  $\phi = 0.9$ . Fig. 3 shows the maximum longitudinal reinforcement ratios,  $\rho_b$ , for a given axial stress and a given concrete cylinder compressive strength at which a rectangular wall panel cracks computed using the above values.

In Fig. 3, it is apparent that an increase in axial compressive stress reduces the maximum value of  $\rho_b$ . This is because an increase in axial compression increases the moment capacity, which is greater than the cracking moment increase.

Limitations to the longitudinal bar diameter,  $d_b$ , connecting the wall panels are advisable. On the one hand, the bar diameter should not be too large to avoid splitting of the wall panel and yet not too small to limit the yield strain penetration and, therefore, the wall's lateral deformation capacity. For these reasons, the ratio of wall thickness,  $t_w$ , to bar diameter,  $d_b$ , should be such that  $9 \leq t_w/d_b \leq 15$ .

### Design for Shear

The critical region for shear in this precast system is at the base of the walls, where an opening of the connection is expected to occur. Most of the shear force resisted across the connection is transferred by friction between the wall panel and the foundation and, to a lesser extent, by dowel action in the reinforcing bars crossing the connection. A small component of the shear force is transferred by kinking in the longitudinal bars crossing the connection.<sup>8</sup>

The former two mechanisms can be assumed to carry the entire shear force. If these mechanisms are assumed to be additive and independent, the shear force resisted at the connection,  $V_n$ , can be expressed as:

$$V_n = V_d + V_f \quad (1)$$

where  $V_d$  and  $V_f$  are the components of the shear force carried by dowel action and friction, respectively.

It is worth noting that the peak value of  $V_n$  does not result from the sum of the peak values of each of the resisting mechanisms since these mechanisms do not reach their peak values simultaneously.

The shear force carried by dowel action,  $V_d$ , is equal to the horizontal component of the axial forces that develop once sliding shear occurs between the jointing surfaces. This force is mathematically expressed as:

$$V_d = \sum A_{si} f_{si} \sin \kappa_i \quad (2)$$

where  $A_{si}$ ,  $f_{si}$  and  $\kappa_i$  are the area, axial stress and kink angle with respect to the vertical axis of bar  $i$ , respectively. Note that stress  $f_{si}$  is defined positive in tension.

The shear force carried by the friction mechanism is:

$$V_f = \mu_f C_c = \mu_f (N + \sum A_{si} f_{si}) \quad (3)$$

where  $\mu_f$  is the coefficient of friction,  $C_c$  is the compressive force carried by the concrete and  $N$  is the concentric axial force, which is taken positive in compression.

A close inspection of Eqs. (2) and (3) reveals that the wall longitudinal reinforcement in compression, resulting from combined bending and axial load, has a detrimental effect on both the friction and sliding shear resisting mechanisms. This effect is particularly pronounced during reversed cyclic loading. It should be noted, however, that at peak loading, the reinforcement in "compression" in these walls could be nominally in tension depending upon the location of the bars in the wall and the lateral load history.

It is well known that compressive reinforcement is placed in reinforced concrete members to increase the ductility capacity.<sup>8</sup> However, in lightly reinforced walls, the lack of compressive reinforcement has little effect on the flexural and rotational capacities.

An upper bound equation for the bending moment at the development of overstrength,  $M_o$ , for the wall depicted in Fig. 4 is obtained assuming the resultant compressive force,  $C_c$ , is located at the wall panel edge. Thus:

$$M_o \cong \left( \omega_o T_y + \frac{N}{2} \right) l_w \quad (4a)$$

where  $\omega_o$  is the overstrength factor,  $T_y = A_{st} f_y / 2$  is the yield force of the reinforcing bars with area  $A_{st} / 2$  located toward one end of the wall, and  $l_w$  is the length of the wall.

The shear force at the base of the wall corresponding to the development of the flexural overstrength,  $V_o$ , is:

$$V_o = \frac{M_o}{h_{eff}} \quad (4b)$$

where  $h_{eff}$  is the height measured from the base of the wall to the resultant lateral force. For low-rise buildings up to three stories,  $h_{eff}$  can be directly obtained as the height of the resultant base shear force obtained from the static lateral force procedure.

The nominal shear resistance,  $V_n$ , at the wall-foundation connection for walls in which the connection reinforcement is grouped towards the wall ends can be obtained from Eqs. (1) to (3):

$$V_n = \mu_f [(1 + \xi) \omega_o T_y + N] + (1 + \xi) \omega_o T_y \sin \kappa \quad (5)$$

where coefficient  $\xi$  is the ratio between the force in the bars grouped close to the extreme fiber in compression to that of the bars grouped close to the extreme fiber in tension (see Fig. 4).

Coefficient  $\xi$  is sensitive to the location of the bars and to the loading history. For symmetrically reinforced walls subjected to reversed cyclic loading beyond the elastic limit, extreme values for this coefficient are  $\xi = -1$  and  $\xi = 1$ . Unfortunately, these values are found for cases of little practical application. Coefficient  $\xi = -1$  when the bars are placed at the wall ends, whereas  $\xi = 1$  when the bars are placed at the center of the wall.

In practice, reinforcing bars are placed so that  $0.5 \leq g \leq 0.95$ , where  $g$  is the distance between the centroids of the groups of bars as a proportion of the wall length (see Fig. 4). A conservative expression proposed for determining the coefficient  $\xi$  is:

$$\xi = 1 - 2g \quad (6)$$

If a flexural dominated response is to be ensured, the nominal shear resistance at the connection should be equal to or greater than the shear force acting at the connection at the development of overstrength. Thus:

$$\phi_s V_n \leq V_o \quad (7)$$

where  $\phi_s$  is the strength reduction factor for shear, taken equal to 1 in capacity designed structures.<sup>11</sup>

Eqs. (4) and (5) can be combined and solved for  $V_n$ . This expression takes the form:

$$V_n = \mu'_f N \quad (8)$$

where  $\mu'_f$  is an equivalent friction coefficient. This coefficient is given by:

$$\mu'_f = \left[ 1 + \frac{(1 + \xi)}{2} \left( \frac{2e_o}{l_w} - 1 \right) \left( 1 + \frac{\sin \kappa}{\mu_f} \right) \right] \mu_f$$

with  $\mu_f \leq \mu'_f \leq \infty$  (9)

where  $e_o$  is the axial load eccentricity defined as  $e_o = M_o / N$ .

Coefficient  $\mu'_f$  relates the shear force transferred by the friction and dowel action mechanisms as a proportion of the applied axial load.

When  $\kappa = 0$ , the entire shear force is transferred by friction since no sliding shear occurs between the jointing surfaces. The case when  $\mu'_f = \mu_f$  and  $\kappa = 0$  is found only in rocking walls in which no longitudinal reinforcement crosses the connection. Further, the case when  $\mu'_f \rightarrow \infty$  and  $\kappa = 0$  is found in slender walls whose response is dominated by flexure and the shear force is transferred irrespectively from the axial load level.

Eq. (9) can be simplified by considering that the kink angle of the reinforcement in these walls is expected to be small for which  $\sin \kappa = \kappa$ . Thus, Eq. (9) can be rewritten as:

$$\mu'_f = \left[ 1 + \frac{(1 + \xi)}{2} \left( \frac{2e_o}{l_w} - 1 \right) \left( 1 + \frac{\kappa}{\mu_f} \right) \right] \mu_f$$

with  $\mu_f \leq \mu'_f \leq \infty$  (10)

In some cases, particularly in stout walls, Eq. (7) can only be satisfied if

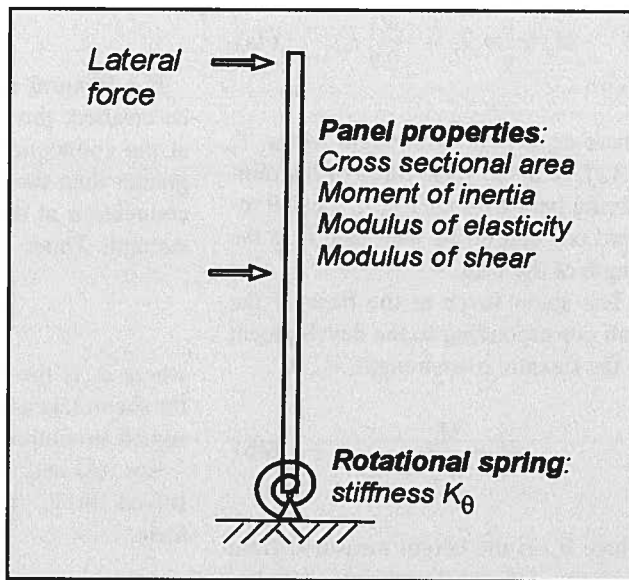


Fig. 5. Proposed analytical model.

and  $l_f$  are the area and length of the rectangular foundation supporting the wall, respectively. Note that the expression developed for  $K_f$  assumes that the foundation and the soil underneath are permanently in contact.

The fixed-end rotation is caused mainly by strain penetration of the tensile reinforcement anchored in the wall panel and in the foundation.<sup>2</sup> In rocking walls, rotation occurs solely due to the compressive strains that develop in the concrete.

To encompass the complete range of walls, the following expression is proposed for  $\theta_j$ :

$$\theta_j = \frac{20d_b f_y}{j l_w E_s} \quad \text{or} \quad \theta_j = \frac{16N}{3E_c A_w} \quad (14)$$

sliding shear is permitted so that a fraction of the shear force is transferred by dowel action. However, it should be noted that sliding shear displacements have two major drawbacks:

First, sliding results in pinching of the hysteretic response if it takes place before the jointing surfaces enter in contact, or in grinding if it occurs after the surfaces enter in contact.

Second, and most importantly, large magnitude sliding shear displacements in walls of different lengths in a multi-story building will result in kinematic incompatibility.

To maintain sliding displacements to within a small component of the lateral displacement at peak loading, the following recommendation is made for the kinking angle  $\kappa$ :

$$\kappa = \frac{1}{3} \left( \frac{2e_o}{l_w} - 1 \right) \text{ radians} \quad (11)$$

with  $0 \leq \kappa \leq 0.2$  radians

### Overall Lateral Force-Lateral Displacement Response

#### Response Within the Elastic Limit

— The evaluation of the seismic actions for this precast system should be performed in accordance with local seismic design provisions. For this evaluation, the design engineer is required to build a suitable mathematical model by modeling the walls with appropriate stiffness values and by deter-

mining the useable displacement ductility in each wall. The useable displacement ductility could be used to estimate the response modification factor required by the relevant building code.

The walls can be represented with the model illustrated in Fig. 5, which combines a prismatic beam element and a rotational spring. The beam element idealizes the wall panel itself. This element can be modeled using elastic theory based on the wall's gross section properties. The rotational spring accounts for flexibility resulting from the opening at the connection as well as from the rotation due to the soil.

The stiffness  $K_\theta$  of this spring is given by:

$$K_\theta = \frac{1}{\frac{1}{K_j} + \frac{1}{K_f}} \quad (12)$$

where the rotational wall-foundation connection stiffness,  $K_j$ , and the foundation rotational stiffness,  $K_f$ , are given by:

$$K_j = \frac{M_j}{\theta_j} \quad \text{and} \quad K_f = \frac{k_m A_f l_f^2}{12} \quad (13)$$

where  $\theta_j$  is the fixed-end rotation at the development of the nominal moment,  $M_n$ , at the base of the wall,  $k_m$  is the soil subgrade reaction modulus,  $A_f$

whichever is greater, where  $d_b$  is the diameter of the connecting bar,  $E_c$  is the concrete elastic modulus, and  $A_w$  is the wall gross section area.

In place of a rational approach involving equilibrium and strain compatibility, the nominal moment,  $M_n$ , in lightly reinforced walls can be approximately calculated as:

$$M_n = \left( T_y + \frac{N}{2} \right) l_w \quad (15)$$

The shear force,  $V$ , corresponding to the nominal moment is given by:

$$V = \frac{M_n}{h_{eff}} \quad (16)$$

and the yield displacement,  $\Delta_y$ , calculated at the height of the resultant lateral force is:

$$\Delta_y = \left\{ \theta_j + \theta_f + \frac{4M_n h_{eff}}{E_c A_w l_w^2} \left[ 1 + \frac{3}{4} \left( \frac{l_w}{h_{eff}} \right)^2 \right] \right\} h_{eff} \quad (17)$$

Eq. (17) considers the three main contributors to the lateral displacement in a cantilever wall loaded with a single lateral force applied at a height  $h_{eff}$ . The first and second terms in Eq. (17) account for the rotation caused by



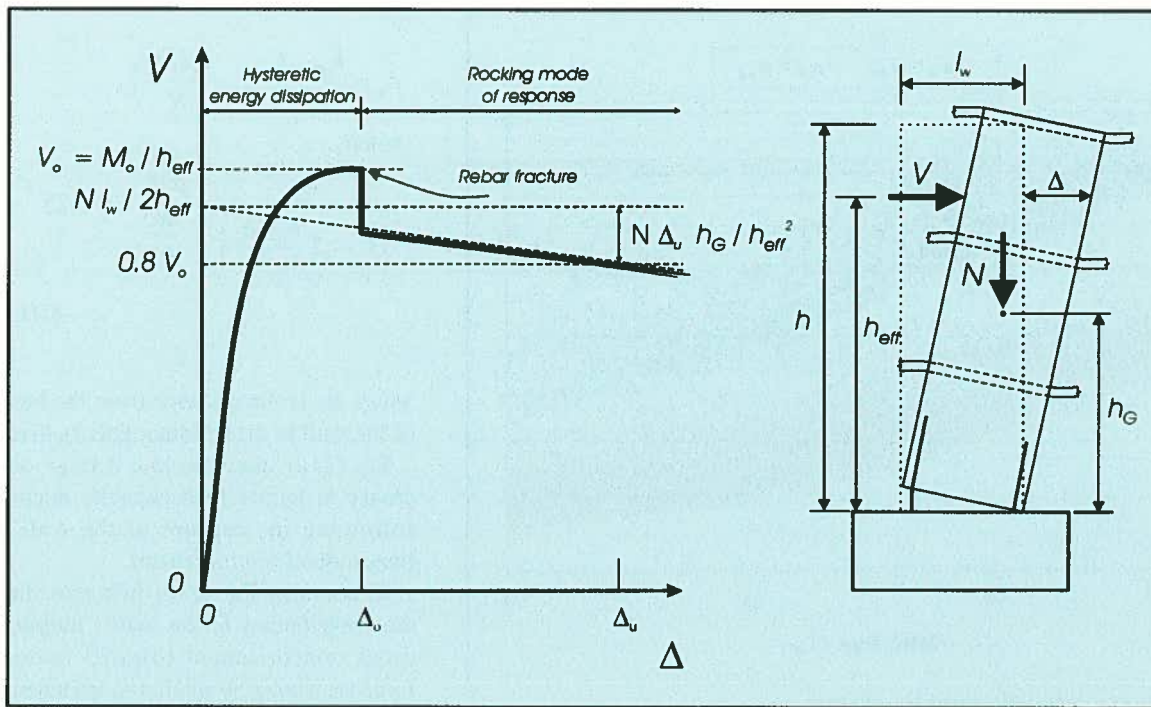


Fig. 6. Lateral force-lateral displacement response of a lightly reinforced precast concrete wall.

opening of the joint and by the foundation flexibility, respectively, whereas the third term accounts for elastic flexure and shear deformations in the uncracked wall panel.

The latter term can be derived using first principles of mechanics while also assuming that the concrete elastic to shear moduli ratio  $E_c/G_c = 2.5$ .<sup>12</sup>

The foundation rotation  $\theta_f$  for use in Eq. (17) is given by:

$$\theta_f = \frac{M_n}{K_f} \quad (18)$$

**Response Beyond the Elastic Limit** — These walls have a lateral force-lateral displacement monotonic response, which is described in Fig. 6. The response of these walls is characterized by two distinct phases:

In the first phase, hysteresis occurs mainly from yielding at the wall-foundation connection. A self-centering response, that is, a response that does not leave residual displacements, is attained when the ratio  $N/(A_w \rho_t f_y) \geq 0.77$ . A large level of energy dissipation per cycle will occur when  $N/(A_w \rho_t f_y) < 0.77$ , but this will occur at the expense of residual displacements.

Upon the development of the nominal flexural strength, the reinforcing bars in the wall-foundation connection

Table 1. Parameters varied in the random simulation.

Variable	Units	Limits	
		Minimum	Maximum
$b_w/d_b$	—	9	16
$f'_c$	psi (MPa)	2900 (20)	5800 (40)
$g$	—	0.5	0.95
$h_{eff}/l_w$	—	1	4
$h_G/h_{eff}$	—	$1/2$	$2/3$
$N/(A_w f'_c)$	—	0	0.04
$\omega_o$	—	1.22	1.62
$\rho_t$	—	0	0.24 percent

undergo strains well into the work hardening region. At some point, mainly due to cyclic loading, these bars fracture after being repeatedly bent back and forth and axially strained up to large tensile strains and back to nearly zero strain. At the point immediately before fracturing of the bars, the wall attains its peak overstrength.

The second phase develops upon fracturing of the reinforcing bars. The response of the wall when laterally loaded beyond this point is well described by the response of a rocking rigid body.

The lateral displacement,  $\Delta_o$ , corresponding to the development of the flexural overstrength and calculated at the effective wall height  $h_{eff}$  can be derived similarly to Eq. (17) if sliding shear displacements across the connection are neglected:

$$\Delta_o = \left\{ \theta_j^o + \theta_f^o + \frac{4M_o h_{eff}}{E_c A_w I_w^2} \left[ 1 + \frac{3}{4} \left( \frac{l_w}{h_{eff}} \right)^2 \right] \right\} h_{eff} \quad (19)$$

where the fixed-end and foundation rotations,  $\theta_j^o$  and  $\theta_f^o$  respectively, are given by:

$$\theta_j^o = \frac{12 d_b \epsilon_{su}^*}{(1+g)l_w/2} \quad \text{and} \quad \theta_f^o = \frac{M_o}{K_f} \quad (20)$$

in which  $\epsilon_{su}^*$  is the effective ultimate tensile strain.

In recognition that cyclic reversed loading results in a reduction of the ul-



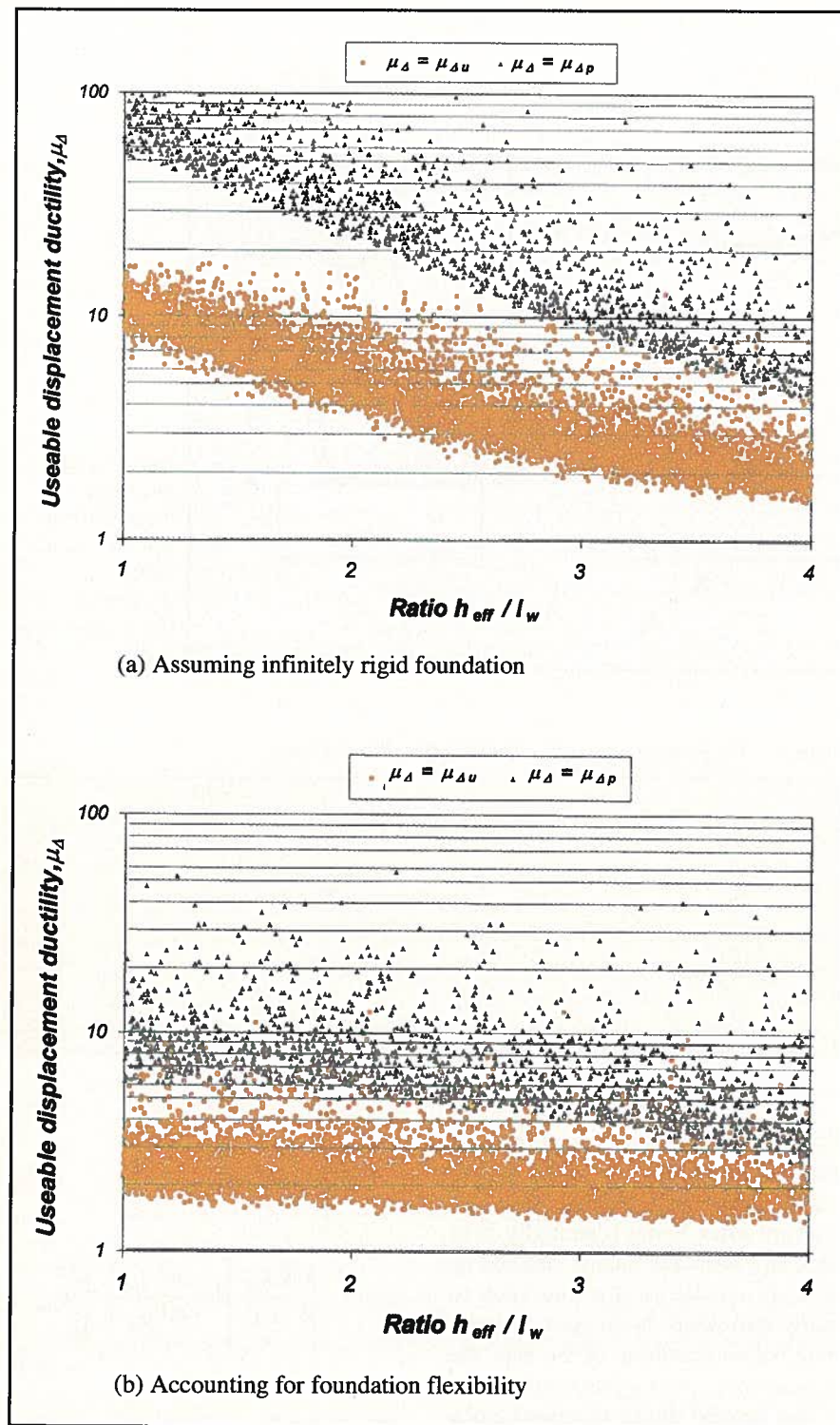


Fig. 7. Useable displacement ductility as a function of the wall aspect ratio.

imate tensile strain for the reinforcing bars, a value of one-half of the ultimate tensile strain obtained from a monotonic tensile test is recommended for  $\epsilon_{su}^*$  for use in design.

The ultimate lateral displacement,  $\Delta_u$ , arbitrarily defined here as the displacement associated with a 20 percent decrease in lateral force resis-

tance from the peak lateral force, can be obtained for these walls as:

$$\Delta_u = \Delta_o \quad \text{when} \quad \frac{\omega_o}{\left(1 - 2 \frac{h_G \Delta_o}{h_{eff} l_w}\right)} \frac{\rho_l f_y}{N} \geq 0.25 \quad (21a)$$

or

$$\Delta_u = \frac{h_{eff}}{h_G} \left( \frac{l_w}{2} - \frac{0.8 M_o}{N} \right)$$

when

$$\frac{\omega_o}{\left(1 - 2 \frac{h_G \Delta_o}{h_{eff} l_w}\right)} \frac{\rho_l f_y}{N} < 0.25 \quad (21b)$$

where  $h_G$  is the distance from the base of the wall to the resultant gravity load.

Eq. (21a) indicates that a large decrease in lateral load capacity occurs following the rupture of the wall's longitudinal reinforcement.

In contrast, Eq. (21b) indicates that the contribution of the wall's longitudinal reinforcement towards lateral force resistance is small and fracturing of these bars only results in a small decrease in the capacity of the wall. Thus, the response of such walls is dominated by rocking. Providing that adequate detailing is provided at the base of these walls, the rocking response could be advantageously used in design.

#### Useable Displacement Ductility —

The concept of useable displacement ductility is introduced in this paper to relate the response of the precast concrete system to a given performance level. The useable displacement ductility,  $\mu_{\Delta}$ , is defined as the lesser of the ultimate displacement ductility,  $\mu_{\Delta u}$ , or the displacement ductility ratio,  $\mu_{\Delta p}$ , corresponding to the lateral displacement associated with the performance level under consideration.

This concept is mathematically expressed as:

$$\mu_{\Delta} \text{ the lesser of } \mu_{\Delta u} \text{ or } \mu_{\Delta p} \quad (22a)$$

where

$$\mu_{\Delta u} = \frac{\Delta_u}{\Delta_y} \quad \text{and} \quad \mu_{\Delta p} = \frac{\Delta_p}{\Delta_y} \quad (22b)$$

and where

$$\Delta_p = \Theta h_{eff} \quad (22c)$$

in which  $\Theta$  is the drift ratio corresponding to the performance level under consideration.

A random variable simulation was performed to illustrate the useable ductility concept in this type of precast concrete wall system. The yield and ultimate displacements,  $\Delta_y$  and  $\Delta_u$ , respectively, were obtained by evaluating Eqs. (17) and (21). Two cases were investigated.

The first case considered fixed-end foundation conditions, that is  $K_f = \infty$ , whereas the other case accounted for the foundation flexibility. In this second case,  $K_f$  was calculated from Eq. (13) with  $l_f/l_w = 1.5$ ,  $A_f/A_w = 5.5$  and with  $k_m = 255 \text{ kip/ft}^3$  ( $40 \text{ MN/m}^3$ ). The parameters, which varied in the study, are listed in Table 1.

The drift ratio chosen for the evaluation of Eq. (22c) was  $\Theta = 0.02$ . The generation of variables was performed using equal probability with values within the limits listed in Table 1 and assuming the connection was reinforced with Grade 60 ksi (414 MPa) bars and that  $\mu_f = 0.7$ . Only those results that resulted in uncracked wall panels and that satisfied Eq. (7) were selected.

The values of  $\mu_\Delta$  obtained from the simulation are plotted against the wall aspect ratio  $h_{eff}/l_w$  in Fig. 7. The results obtained for the case of walls on a rigid foundation are shown in Fig. 7(a), whereas the results obtained considering foundation flexibility are shown in Fig. 7(b).

For those walls on rigid foundations, the system's useable displacement ductility is highly dependent on the wall aspect ratio and on the controlling mode of failure. The useable displacement ductility decreases significantly with the wall aspect ratio. Moreover, walls whose response is dominated by rocking, Eq. (21b), have a greater useable displacement ductility than walls whose response is controlled by the fracture of the longitudinal reinforcement, Eq. (21a), for the same wall aspect ratio.

A comparison of Figs. 7(a) and 7(b) clearly illustrates the effect that foundation flexibility has on the useable displacement ductility. The flexibility of the foundation decreases the useable displacement ductility due to the increase in the yield displacement, which is used to define ductility [see Eqs. (16) and (22b)]. This effect is

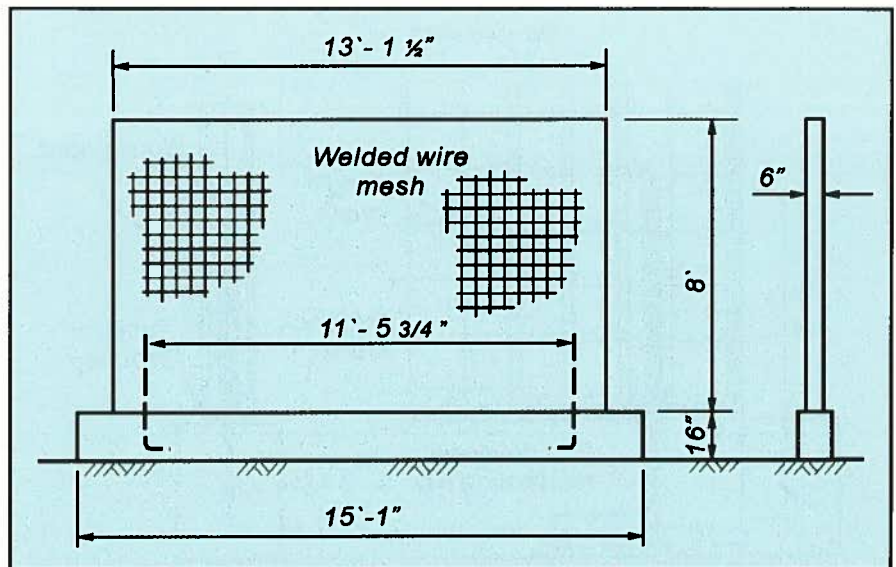


Fig. 8. General dimensions and reinforcing details for test unit.

particularly pronounced in walls with aspect ratios of  $h_{eff}/l_w \leq 3$ .

It is interesting to note that in those walls whose ultimate displacement is defined by Eq. (21a), the useable displacement ductility is fairly independent from the wall aspect ratio and is low in the majority of cases. Since it is generally difficult in practice to attain rigid foundation conditions, it is recommended herein that this precast concrete system be used in conjunction with low response modification factors to ensure nominally elastic or limited ductility response and, hence, to ensure displacement ductility demands that are compatible with the useable displacement ductilities depicted in Fig. 7(b).

This recommendation implies that buildings incorporating this precast concrete jointed wall system should be designed for lateral forces larger than those used in the design of ductile lateral force resisting systems. However, the abundance of walls present in buildings incorporating this system generally results in ultimate moments that can be satisfied with nominal longitudinal reinforcement using the procedure described above. The main attraction of this system is the ease and simplicity in the reinforcing detailing, as no confinement of the concrete or special transverse reinforcement is required in the wall panels.

Larger response modification factors could be used for this system

when the response of the walls is controlled by rocking. The evaluation of the response modification factors for this particular case and the design of a foundation system to ensure a suitable rocking response are outside the scope of this paper.

## EXPERIMENTAL WORK

This section provides a general description of the test unit, describes the test arrangement and material properties of the specimens, and gives the general and lateral force-displacement responses.

### General Description of the Test Unit

A full-scale test unit representing an example of the jointed system in a two-story building was built and tested under reverse cyclic loading. Fig. 8 illustrates the overall dimensions of the test unit and Fig. 9 depicts the reinforcing details at the bottom corners of the wall panels. The connection at the wall-foundation connection was provided by two 0.6 in. (16 mm) diameter reinforcing bars with a nominal bar area  $A_b = 0.31 \text{ sq in.}$  ( $201 \text{ mm}^2$ ) and a nominal yield strength of 62.4 ksi (430 MPa).

The reinforcing ratio at the connection was  $\rho_t = 0.067$  percent, which is well below that required for cast-in-place wall construction.<sup>9,10</sup> Except for



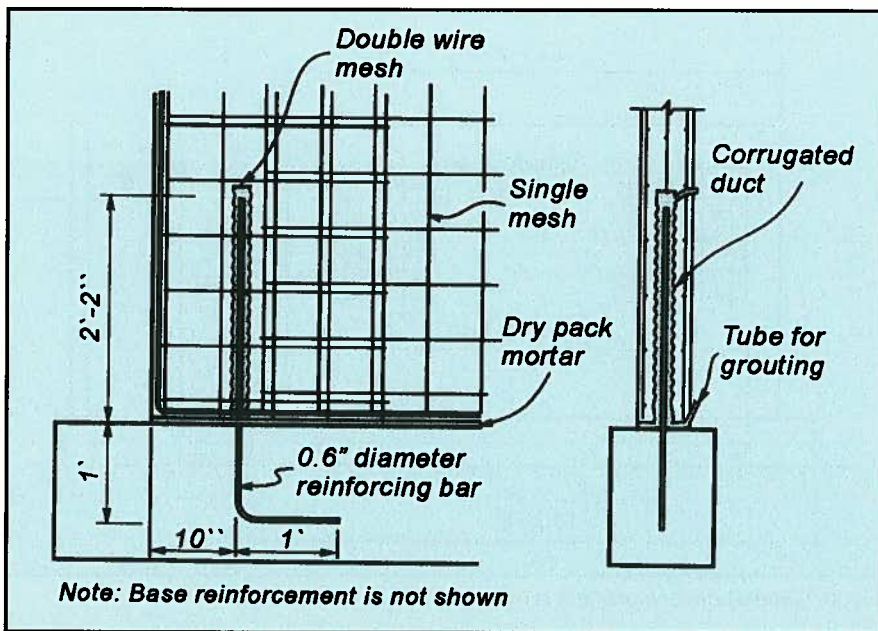


Fig. 9. Connection detail between wall and foundation.

the region around the corrugated ducts, where two layers of welded wire mesh were used, the wall panel was reinforced with a central layer of welded wire mesh, 0.25 in. (6.3 mm) diameter wire at a 6 in. (150 mm) spacing.

In addition, 0.5 in. (12 mm) diameter bars were provided at the perimeter of the wall panel. Corrugated steel ducts, 2 in. (50.8 mm) in diameter and 25.6 in. (650 mm) high, were placed at the bottom of the wall panel to permit the connection of the wall and the foundation beam. At the bottom edge

of the wall panel, two 0.5 in. (12 mm) reinforcing bars were located at each side of the corrugated ducts.

The top face of the reinforced concrete foundation beam was roughened by forming criss-cross grooves when the concrete was in a semi-hardened state. The bottom face of the wall panel was mechanically roughened before erecting the unit.

In order to ensure a uniform thickness of the gap between the panels and the base, 0.2 in. (5 mm) steel shims were placed on the base, and the surface was covered with dry pack mor-

tar. Then, the wall panel was lifted with a crane and located on the reinforced concrete base. Subsequently, each corrugated duct was gravity filled with non-shrinkage grout through a small tube located at the bottom.

### Test Arrangement

The general details of the loading frame are illustrated in Fig. 10. Lateral forces were applied using two hydraulic actuators, which were used to pull alternatively depending on the direction of the applied force. Vertical forces were also applied with servo-controlled hydraulic actuators acting at the top of the panel. These actuators provided a pair corresponding to the overturning moment in the prototype wall at 7 ft (2.1 m) from its base due to the resultant lateral force applied at an effective height of  $h_{eff} = 13$  ft 1 in. (4.55 m) (see Fig. 11).

The axial load acting at the ground level connection was only due to the self-weight of the wall panel of 7.8 kips (34.6 kN). Even though the axial load in the actual precast concrete wall panels is expected to be higher, this case represents an unfavorable condition for the connection because the shear strength of the panel is a function of the axial load.

### Material Properties

The compressive strength of the concrete, measured using 6 in. (150 mm) high x 4 in. (100 mm) diameter cylinders, was 2450 psi (16.9 MPa) at 28 days. The grout pumped into the corrugated steel ducts had a compressive strength of 8350 psi (57.6 MPa) at 28 days.

It was not possible to make specimens for compression tests with the dry pack mortar because this material had a very low water content. However, a sample of this material was taken from the unit after the test was finished. Small prisms 0.63 in. square x 1.26 in. long (16 mm square x 32 mm long) were cut and tested in compression, resulting in a compressive strength of 835 psi (5.8 MPa).

The poor strength of the dry pack mortar could have been due to the poor hydration of the cement caused by the low amount of water used for

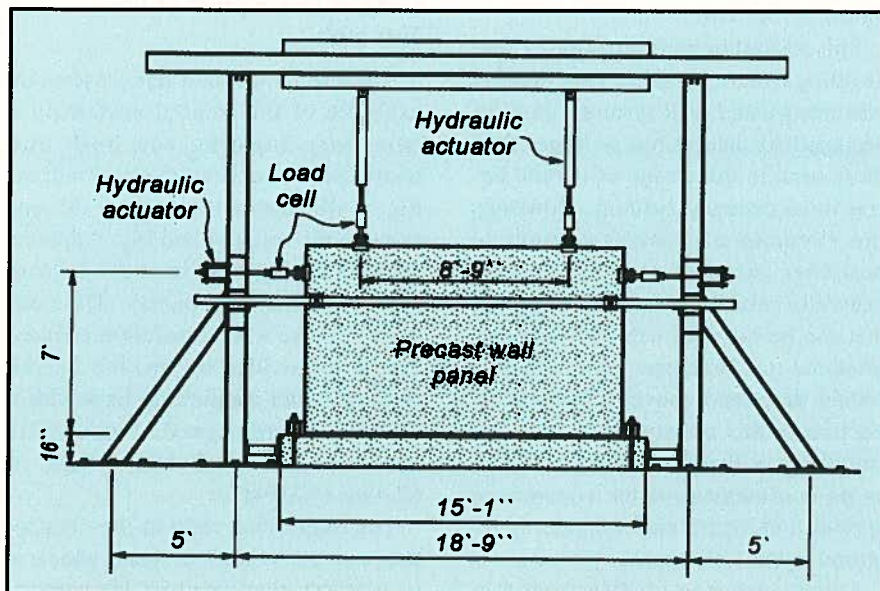


Fig. 10. Test arrangement.

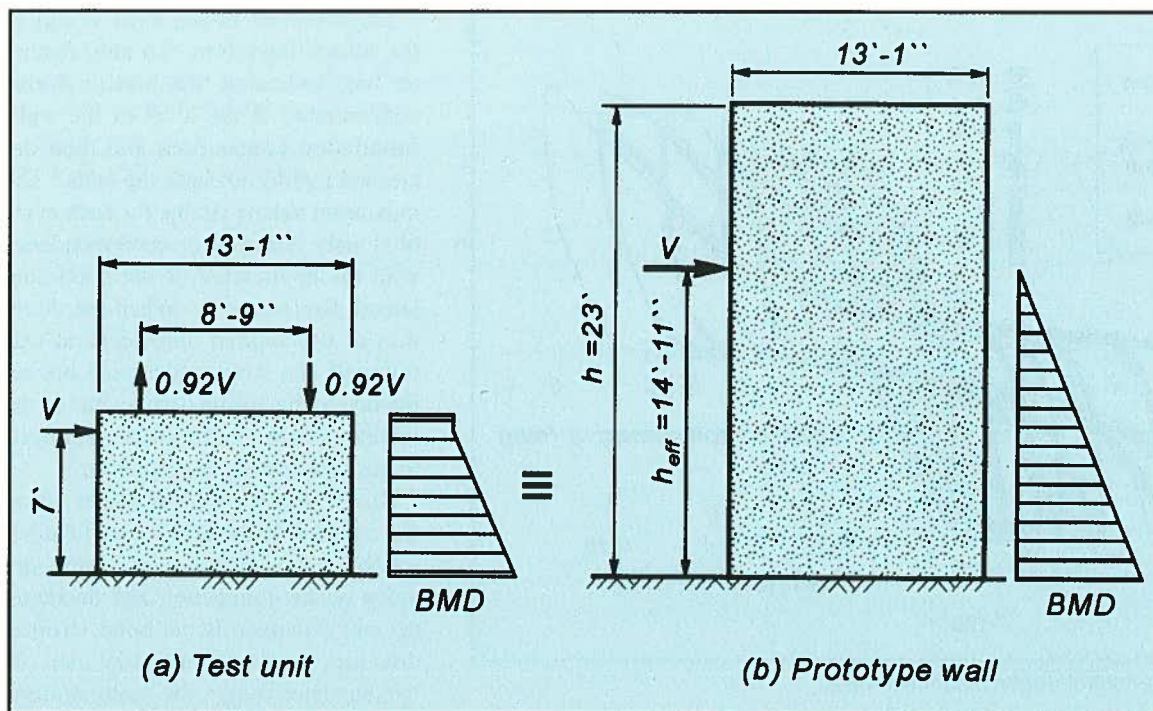


Fig. 11. Loading simulation in test unit.

mixing, which was prepared according to the specifications provided by the manufacturer. The wire mesh and the 0.6 in. (16 mm) diameter bars used in the ground level connection had a yield strength of 65 and 66 ksi (458 and 467 MPa), respectively.

### General Response

Horizontal cracks extending from the extreme fiber in tension toward the center of the wall appeared in the wall-foundation connection during the first cycle. In the second cycle, the cracks propagated beyond the center of the wall panel and intersected the crack developed in the previous semi-cycle. As a result, the entire connection was crossed by a single crack.

As the test continued, a small vertical crack developed at the left edge of the wall along the line of the reinforcing bar that was subjected to tension. This crack developed due to the shear force resisted by the bar by dowel action. The crack did not widen due to the presence of 0.47 in. (12 mm) trimming bars and of the mesh surrounding the connecting reinforcement. The test continued by applying successive cycles of increasing displacement ductility.

In the cycles near the end of the test, sliding displacements in the connection were clearly visible. Such dis-

placements caused grinding of the dry-pack mortar bedding and resulted in crushing. The test was ended after the application of 24 cycles up to a displacement ductility of 7 and a drift ratio of 0.18 percent. At the end of the test, no cracking or any other damage had been observed in the precast wall.

### Lateral Force-Displacement Response

The lateral force versus displacement response of the wall unit is plotted in Fig. 12. The first cycles, theoretically in the "elastic range," exhibited nonlinear inelastic behavior, mainly due to the gradual opening at the connection. The displacements in the positive direction were larger than those in the negative direction, at the same force level, which led to an unsymmetrical response of the unit.

This behavior was probably due to errors in the measurement of the very small lateral displacements and to unsymmetrical sliding of the wall panel. The theoretical response obtained from Eqs. (17) to (19) with  $\theta_f = \theta_f^p = 0$  is also plotted in Fig. 12. The measured initial stiffness of the test unit was significantly lower than indicated theoretically.

The main reason for this difference was the flexibility of the foundation.

As explained before, foundation flexibility has a very large effect on the definition of yield displacement, which is particularly important in this unit because of the small wall aspect ratio of  $h_{eff}/l_w = 1.13$ . Note, however, that there is good agreement between the experimental and theoretical post-elastic response.

Measurements taken from the strain gauges indicated that the connecting bar yielded in tension during the application of 18.3 kips (81.3 kN) in the forward (positive) direction during the third cycle. In the initial cycles beyond the elastic limit, the load-displacement response showed some indications of pinching, but the hysteretic loops still showed reasonable energy dissipation capacity. This pinching effect gradually increased in the following cycles as a result of sliding shear occurring at the wall-foundation connection.

The reloading branch of the hysteresis loops clearly exhibited two different parts. When reloading started, the wall panel slid several millimeters with very low resistance and reduced stiffness. This behavior was expected as the ratio  $N/(A_w \rho_t f_y)$  for this unit was only 0.18, which indicates that, upon unloading, the axial force was unable to yield the bars back to zero strain and, thus, to close the gap in the connection.



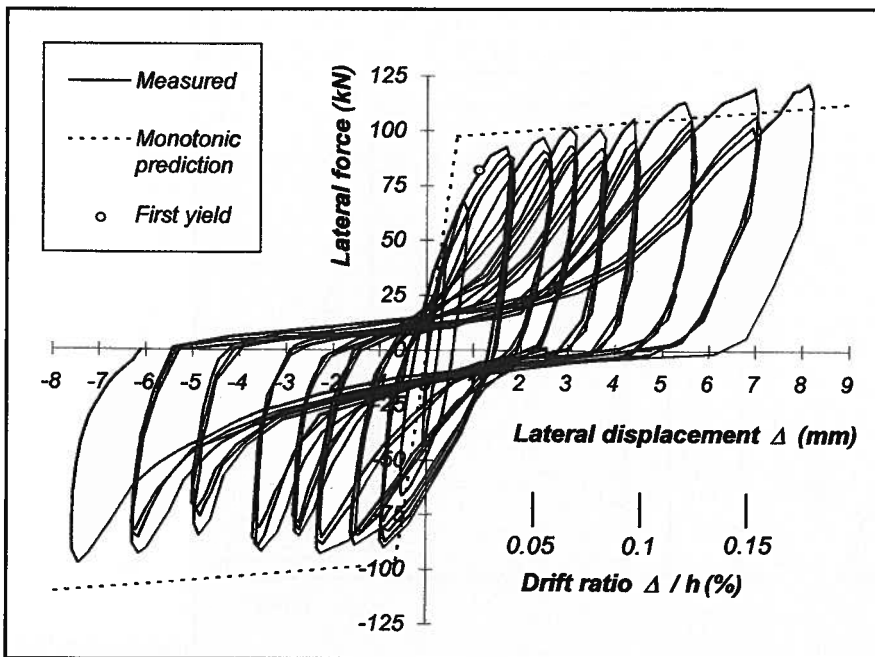


Fig. 12. Lateral force-lateral displacement response.

An increase in both stiffness and strength was observed once the jointing surfaces contacted and enabled the friction mechanism of shear transfer. The repetition of cycles to equal displacement ductilities was accompanied by a decrease in the lateral strength. Moreover, the hysteresis loop exhibited stiffness degradation in the reloading branches. These effects were usually more significant between the first and second cycle of the series.

The horizontal displacement measured at the point of application of the lateral force can be divided into four components related to:

1. Elongation of the reinforcing bars at the wall-foundation connection.
2. Flexural and shear deformations in the precast walls.
3. Sliding shear at the wall-foundation connection.
4. Rigid body movements originated by sliding or rotation of the foundation.

Analytical calculations indicate that, by comparison, shear and flexural deformations in the walls are small due to the large stiffness of the wall compared to that of the ground level connection. This conclusion was experimentally verified in a similar test on two coupled precast walls.<sup>2</sup>

The analysis of the results shows

that sliding shear became the controlling mode of deformation, especially when large displacements were imposed, as a result of the degradation of the frictional mechanism at the panel-base interface. Sliding shear had a significant influence on the response of the unit and accounted for more than 50 percent of the lateral displacement in the cycles near the end of the test.

The coefficient of friction,  $\mu_f$ , at the panel-base interface from Cycles 1, 2 and 3 was 0.70, 0.69 and 0.71, respectively. In order to calculate these values, the clamping action was evaluated taking into account the stresses developing in the reinforcing bars when the peak load was applied. Sliding shear displacements in these cycles were less than 1/127 in. (0.2 mm) which suggest that the contribution to shear resistance from dowel action could be ignored.

The analysis of the experimental results indicates that the friction mechanism degraded as a result of grinding of the dry-pack mortar bedding, which resulted in the accumulation of small particles resulting in a rolling mechanism. Analysis of the data showed that when sliding displacements had resulted in a kinking angle  $\kappa = 10$  degrees (0.17 radians), the friction coefficient had decreased from the initial average value of 0.7 to 0.51.

Measurement of the local strains in the connecting 0.6 in. (16 mm) diameter bars indicated that plastic strains concentrated at the level of the wall-foundation connection, and then decreased rapidly towards the ends.<sup>2</sup> The maximum tensile strains for each cycle obviously occurred in correspondence with the application of the maximum lateral displacements. When the direction of the applied displacement was reversed, the strains decreased but remained in the tensile domain due to the inability of the axial compression force to push them back to zero strain.<sup>2</sup>

Strain measurements taken along the connecting 0.6 in. (16 mm) diameter bars indicate that peak strains develop at the connection and decrease, up and downwards, as bond stresses develop, somewhat linearly over 20 bar diameters when the yield strength of the bar is attained.<sup>2</sup> Measurements also showed that, at large strains, the large strain concentration occurred over a much shorter length, of about 12 bar diameters.<sup>2</sup> These two observations were used to derive the rotations in Eqs. (14) and (20), respectively.

## CONCLUSIONS

Based on the results of this investigation, the following conclusions can be drawn:

1. A jointed precast concrete wall system can be designed to provide lateral force resistance in high seismic regions. The system is very lightly reinforced, with longitudinal steel ratios at the wall-foundation connection that are less than those required for cast-in-place wall construction. The system is intended for use in low-rise building construction with an abundant number of walls. The main attractions of this system are the ease of the reinforcing details in the wall panels and the lack of earthquake-induced structural damage in the wall panels themselves.

2. In this system, the vertical bars protruding from the foundation are grouted into the precast concrete wall. The precast wall units are lowered into position, ensuring that the bars protruding from the foundation beam are anchored into galvanized corrugated steel ducts a distance at least equal to the development length.

3. A nonlinear lateral force-lateral displacement response results in this system from opening of the wall-foundation connection. Energy dissipation results from yielding of the reinforcing bars crossing the connection while ensuring sliding shear in the connection is minimized and cracking in the wall panels is avoided. The design with this system requires the use of ductile reinforcement in the connection region. It is recommended that the ultimate tensile strain, that is, the tensile strain at the ultimate tensile strength, should not be less than 12 percent to avoid premature bar fracture at the wall-foundation connection.

4. The theoretical aspects relevant to the seismic design and behavior of this precast concrete system are described in the paper. In particular, emphasis is given to the evaluation of the

system's stiffness, lateral displacement and ductility, and to the shear transfer at the connection. It is shown that the foundation flexibility has a large effect in the useable ductility, particularly when low aspect ratio walls are used.

5. In order to keep the displacement ductility demands compatible with the useable displacement ductility, lateral forces should be determined using reasonably low response modification factors to ensure limited ductility system response.

6. Experimental work was conducted to assess the response of such a system. A full-scale wall unit was built and tested under reversed cyclic loading. The test was conclusive in showing that precast concrete wall panels with a horizontal construction joint at the base of the wall can be designed

for limited ductility response, when the design ensures that the ultimate flexural strength at the wall-foundation beam connection is less than the cracking moment of the wall panel. This is because the plasticity concentrates at the connection region and is unable to spread through the wall panel.

## ACKNOWLEDGMENT

The Foundation for Research, Science and Technology, New Zealand, is gratefully acknowledged for granting the funding from the Public Good Science Fund (Contract UOC 306, 1993/96) that made this research program possible.

The authors would like to express their appreciation to the PCI JOURNAL reviewers for their most helpful suggestions and constructive comments.

## REFERENCES

1. *Guidelines for the Use of Precast Concrete in Buildings*, Report of a Study Group of the New Zealand Concrete Society and the New Zealand Society for Earthquake Engineering, Second Edition, Centre for Advanced Engineering, University of Canterbury, Christchurch, New Zealand, December 1999, 144 pp.
2. Restrepo, J. I., Crisafulli, F. J., and Park, R., "Earthquake Resistance of Structures: The Design and Construction of Tilt-Up Reinforced Concrete Buildings," Research Report 96-11, Department of Civil Engineering, University of Canterbury, Christchurch, New Zealand, 1996.
3. Holden, T. J., Restrepo, J. I., and Mander, J. B., "Seismic Performance of Precast Reinforced and Prestressed Concrete Walls," *Journal of Structural Engineering*, American Society of Civil Engineers, in press.
4. Anderson, A. R., "Composite Designs in Precast and Cast-in-Place Concrete," *Progressive Architecture*, September 1960, pp. 172-179.
5. Mast, R. F., "Auxiliary Reinforcement in Concrete Connections," Proceedings of the American Society of Civil Engineers, *Journal of the Structural Division*, V. 94, ST6, June 1968, pp. 1485-1504.
6. Paulay, T., Park, R., and Phillips, M. H., "Horizontal Construction Joints in Cast-in-Place Concrete," *Shear in Reinforced Concrete*, ACI Special Publication SP-42, V. 2, Farmington Hills, MI, 1974, pp. 599-616.
7. Soudki, K. A., West, J. S., Rizkalla, S. H., and Blackett, B., "Horizontal Connections for Precast Concrete Shear Wall Panels Under Cyclic Shear Loading," *PCI JOURNAL*, V. 41, No. 3, May-June 1996, pp. 64-80.
8. Park, R., and Paulay, T., *Reinforced Concrete Structures*, John Wiley & Sons, Inc., New York, NY, 1975.
9. NZS 3101, *Concrete Structures Standard, Part 1: The Design of Concrete Structures and Part 2: Commentary on the Design of Concrete Structures*, Standards Association of New Zealand, Wellington, New Zealand, 1995.
10. ACI Committee 318, "Building Code Requirements for Structural Concrete (ACI 318-95) and Commentary (ACI 318R-95)," American Concrete Institute, Farmington Hills, MI, 1995.
11. Paulay, T., and Priestley, M. J. N., *Seismic Design of Reinforced Concrete and Masonry Buildings*, John Wiley & Sons, Inc., New York, NY, 1992.
12. Popov, E., *Mechanics of Materials*, Prentice-Hall Inc., Second Edition, Englewood Cliffs, NJ, 1978.



## APPENDIX A — NOTATION

<p> <math>A_f</math> = foundation area  <math>A_{si}</math> = area of reinforcing bars  <math>A_{st}</math> = total area of reinforcement  <math>A_w</math> = gross cross-sectional area of wall  <math>C_c</math> = compressive force carried by concrete  <math>d_b</math> = reinforcing bar diameter  <math>e_o</math> = axial load eccentricity defined as <math>M_o/N</math>  <math>E_c</math> = concrete elastic modulus  <math>E_s</math> = steel elastic modulus  <math>f'_c</math> = concrete cylinder compressive strength  <math>f_{si}</math> = steel stress  <math>f_y</math> = yield strength of reinforcing steel  <math>g</math> = distance between centroids of groups of bars as a proportion of wall length  <math>G_c</math> = concrete shear modulus  <math>h</math> = overall wall height  <math>h_{eff}</math> = height from wall base to resultant of horizontal seismic force  <math>h_G</math> = height from wall base to centroid of gravity force  <math>k_m</math> = soil subgrade reaction modulus  <math>K_f</math> = foundation rotational stiffness  <math>K_j</math> = wall-foundation connection rotational stiffness  <math>K_\theta</math> = rotational stiffness  <math>l_f</math> = foundation length  <math>l_w</math> = wall length  <math>M_o</math> = flexural overstrength  <math>M_n</math> = nominal flexural strength  <math>M_r</math> = moment capacity of rigid rocking block  <math>N</math> = concentric axial load  <math>t_w</math> = wall thickness  <math>T_y</math> = yield force of group of bars                 </p>	<p> <math>V_n</math> = nominal shear strength  <math>V_o</math> = shear force in wall corresponding to development of flexural overstrength at connection  <math>w_f</math> = foundation width  <math>\Delta</math> = wall lateral displacement at effective height, <math>h_{eff}</math>  <math>\Delta_o</math> = lateral displacement at development of flexural overstrength  <math>\Delta_p</math> = lateral displacement at effective height, <math>h_{eff}</math>, corresponding to performance limit  <math>\Delta_u</math> = ultimate lateral displacement at effective height, <math>h_{eff}</math>  <math>\Delta_y</math> = wall yield displacement at effective height, <math>h_{eff}</math>  <math>\epsilon_{su}^*</math> = effective ultimate tensile strain  <math>\theta_f</math> = foundation rotation at development of nominal strength  <math>\theta_j</math> = fixed-end rotation at wall-foundation connection at development of nominal strength  <math>\theta_f^\circ</math> = foundation rotation at development of overstrength  <math>\theta_j^\circ</math> = fixed-end rotation at wall-foundation connection at development of overstrength  <math>\Theta</math> = drift ratio  <math>\kappa</math> = kink angle  <math>\mu_f</math> = friction coefficient  <math>\mu'_f</math> = equivalent friction coefficient  <math>\mu_\Delta</math> = useable displacement ductility  <math>\mu_{\Delta p}</math> = displacement ductility corresponding to given drift ratio <math>\Theta</math>  <math>\mu_{\Delta u}</math> = displacement ductility capacity  <math>\rho_t</math> = reinforcement ratio  <math>\phi</math> = strength reduction factor for flexure  <math>\phi_s</math> = strength reduction factor for shear  <math>\omega_o</math> = overstrength factor                 </p>
--	---

## APPENDIX B — DERIVATION OF EQUATIONS (9) AND (21)

### Equation (9)

From Eq. (5):

$$\frac{V_n}{N} = \mu_f \left( 1 + (1 + \xi) \frac{\omega_o T_y}{N} \right) \left( 1 + \frac{\sin \kappa}{\mu_f} \right) \quad (\text{B1})$$

Now solving  $\omega_o T_y$  from Eq. (4) and substituting in Eq. (B1):

$$\frac{V_n}{N} = \left[ 1 + \frac{(1 + \xi)}{2} \left( \frac{2e_o}{l_w} - 1 \right) \left( 1 + \frac{\sin \kappa}{\mu_f} \right) \right] \mu_f \quad (\text{B2})$$

But:

$$\frac{V_n}{N} = \mu'_f \quad (\text{B3})$$

Hence:

$$\mu'_f = \left[ 1 + \frac{(1 + \xi)}{2} \left( \frac{2e_o}{l_w} - 1 \right) \left( 1 + \frac{\sin \kappa}{\mu_f} \right) \right] \mu_f \quad (9)$$

### Equation (21)

The moment capacity of a rigid block rocking about its edge,  $M_r$ , is given by:

$$M_r = N \left( \frac{l_w}{2} - \frac{h_G}{h_{eff}} \Delta_o \right) \quad (\text{B4})$$

If the P-Delta effect is accounted for, the moment  $M_o$  of a rigid reinforced concrete rectangular wall can be defined as:

$$M_o = M_r + \omega_o \rho_t f_y b_w \frac{l_w}{2} \quad (\text{B5})$$

If all the longitudinal bars are conservatively assumed to fracture simultaneously, the moment capacity at the base of the wall will suddenly decrease from the peak moment  $M_o$

to  $M_r$ . Failure is considered to occur when the ratio  $M_r/M_o \leq 0.8$ . If this ratio is greater than 0.8, the walls will display a rocking mode of response, for which appropriate measures should be taken in design to ensure suitable behavior under this mode. Hence:

$$\frac{M_r}{M_o} > 0.8 \Rightarrow \text{Drift controlled} \quad (\text{B6a})$$

$$\frac{M_r}{M_o} \leq 0.8 \Rightarrow \text{Strength controlled} \quad (\text{B6b})$$

Substituting Eqs. (B4) and (B5) in Eq. (B6a) yields:

$$\frac{1}{1 + \frac{\omega_o \rho_t f_y}{\frac{N}{A_w} \left( 1 - \frac{2h_G \Delta_o}{h_{eff} l_w} \right)}} > 0.8 \quad (\text{B7})$$

Therefore:

$$\frac{\omega_o}{\left( 1 - \frac{2h_G \Delta_o}{h_{eff} l_w} \right)} \frac{\rho_t f_y}{\frac{N}{A_w}} < 0.25 \quad (21b)$$

From Fig. 6:

$$N \Delta_u \frac{h_G}{h_{eff}^2} = \frac{N l_w}{2 h_{eff}} - 0.8 V_o \quad (\text{B8})$$

But:

$$V_o = \frac{M_o}{h_{eff}} \quad (\text{B9})$$

Substituting Eq. (B9) in Eq. (B8) and solving for  $\Delta_u$ :

$$\Delta_u = \frac{h_{eff}}{h_G} \left( \frac{l_w}{2} - \frac{0.8 M_o}{N} \right) \quad (21b)$$



## APPENDIX C — DESIGN EXAMPLE

The example presented in this appendix describes the use of the design method discussed in this paper. For simplicity, only the design of the walls will be performed for the load combination  $0.9D \pm E$ , where  $D$  and  $E$  are the dead and earthquake loading.

The three-story residential building with plan view shown in Fig. C1 incorporates ten long precast concrete walls as the vertical and lateral force resisting system in both the long and short directions. The walls in the long direction of the building are 10 in. (254 mm) thick x 19 ft 8 in. (6.0 m) long. In the short direction, the walls are 8 in. (203 mm) thick x 19 ft 8 in. (6.0 m) long.

The building is located in a region of high seismic risk for which the base shear to seismic weight ratio, calculated using a response modification factor  $R = 2.5$ , is  $V/W = 0.55$  and  $h_{eff} = 19.35$  ft (5.9 m). The wall-foundation connection and the ducts will be grouted with a high strength shrinkage compensating grout for which a friction coefficient  $\mu_f = 0.7$ .

It is required to design the connection of Walls 1 and 2 if  $f_y = 60$  ksi (414 MPa).

### Design of Longitudinal Reinforcement

The design forces for Walls 1 and 2 for the load combination  $0.9D \pm E$  are summarized in Table C1.

The area of longitudinal reinforcement at the wall-foundation connection can be found from Eq. (15) so that  $\phi M_n \geq M$ . Using  $\phi = 0.9$  and  $f_y = 60$  ksi (414 MPa) and solving for  $T_y$ :

For Wall 1,  $T_y \geq 78.7$  kips (350 kN) and for Wall 2,  $T_y \geq 20.5$  kips (91.1 kN)

But  $T_y = A_{st}f_y/2$ , hence:

For Wall 1,  $A_{st} \geq 2.62$  sq in. (1692 mm<sup>2</sup>) and for Wall 2  $A_{st} \geq 0.68$  sq in. (440 mm<sup>2</sup>).

Therefore, use three #6 bars for Wall 1 ( $A_{st} = 2.64$  sq in.) and two #6 bars for Wall 2 ( $A_{st} = 0.88$  sq in.). Note that the wall thickness-to-bar diameter is  $t_w/d_b = 13.3$  and  $t_w/d_b = 10.7$  for Walls 1 and 2, respectively, which is within the recommended limits of  $9 \leq t_w/d_b \leq 15$ .

### Explicit Capacity Design Checks

Assume that the overstrength factor for the reinforcing bars is  $\omega_o = 1.45$ .

#### 1. Determine the concrete cylinder strength to ensure the walls remain uncracked.

The longitudinal reinforcement ratio at the connection for Wall 1 is:

$$\begin{aligned} \rho_l &= A_{st}/A_w = 2.64/[10 \times (19 \times 12 + 8)] \\ &= 0.11 \text{ percent} \end{aligned}$$

The axial stress is:

$$\begin{aligned} N/A_w &= 127 \times 10^3/[10 \times (19 \times 12 + 8)] \\ &= 58.8 \text{ psi (0.41 MPa)} \end{aligned}$$

For Wall 2,  $\rho_l = 0.046$  percent and  $N/A_w = 97.2$  psi (0.67 MPa).

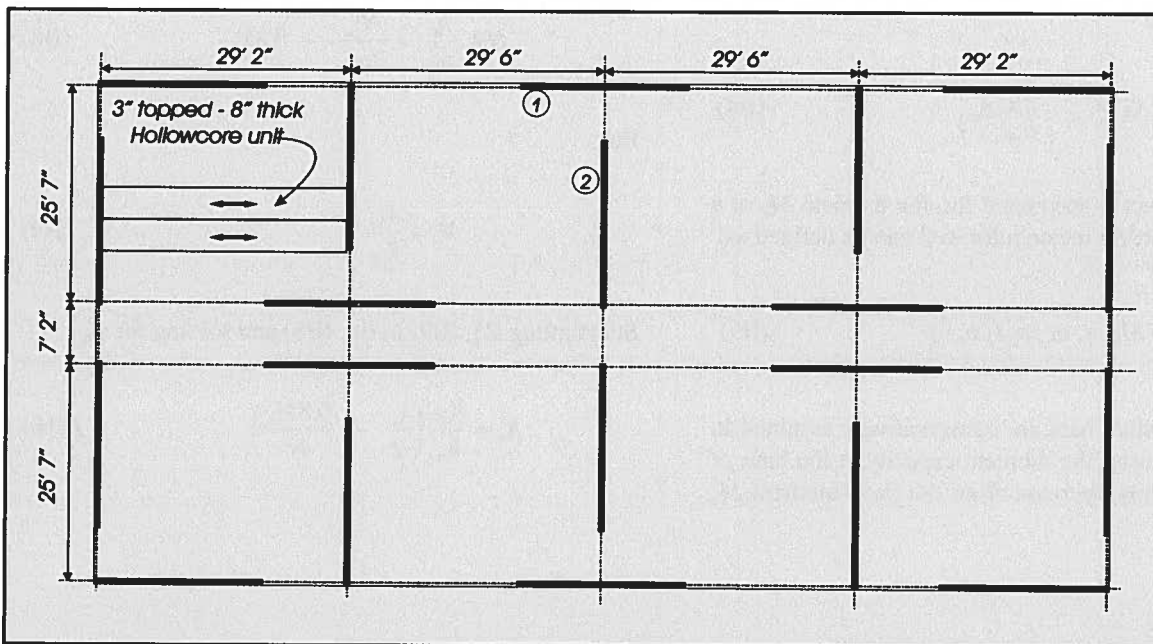


Fig. C1. Typical plan view of building of design example.

Fig. 3 plots the  $(N/A_w$  and  $\rho_t)$  points for Walls 1 and 2. It can be deduced from this plot that a concrete strength with  $f'_c = 4350$  psi (30 MPa) ensures that the wall panels will remain uncracked at the development of the flexural overstrength.

**2. Check the shear transfer at the connection.**

For Wall 1:

The overstrength moment,  $M_o$ , is found from Eq. (4a):

$$M_o = [1.45 \times 2.64 \times 60/2 + 115/2] \times (19 + 8/12) = 3389 \text{ kip-ft (4596 kN-m)}$$

The axial load eccentricity is  $e_o = M_o/N = 3389/115 = 29.5$  ft (9.0 m).

The kink angle,  $\kappa$ , is found from Eq. (11):

$$\kappa = [2 \times 29.5 / (19 + 8/12) - 1] / 3 = 0.667 \text{ radians or } \kappa = 0.2 \text{ radians, whichever is less. Hence, } \kappa = 0.2 \text{ radians.}$$

Try  $g = 0.5$ . Hence, from Eq. (6),  $\xi = 0$ .

Now, the equivalent friction coefficient,  $\mu'_f$ , is determined from Eq. (10):

$$\mu'_f = \left[ 1 + \frac{(1 + 0)}{2} \left( \frac{2 \times 29.5}{19 + 8/12} - 1 \right) \left( 1 + \frac{0.2}{0.7} \right) \right] \times 0.7 = 1.60$$

Table C1. Design forces for Walls 1 and 2 for load combination  $0.9D \pm E$ .

Wall No.	Shear, $V$		Moment, $M$		Axial force, $N$	
	kips	kN	kip-ft	KN-m	kips	kN
1	124	552	2408	3267	115	510
2	124	552	2408	3267	231	1028

The nominal shear force resisted by connection,  $V_n$ , is found from Eq. (8):

$$V_n = 1.60 \times 115 = 184 \text{ kips (819 kN)}$$

Now, the shear force at the development of overstrength,  $V_o$ , is calculated from Eq. (4b):

$$V_o = 3389/19.35 = 175 \text{ kips (778 kN)}$$

Now from Eq. (7) with  $\phi_s = 1$ :

$$\phi_s V_n > V_o \text{ is satisfactory.}$$

For Wall 2, the same procedure yields for  $g = 0.915$ .

$\mu'_f = 0.72$ ,  $\phi_s V_n = 167$  kips (743 kN) and  $V_o = 156$  kips (694 kN).

Hence,  $\phi_s V_n > V_o$  is satisfactory.

The position of the ducts in the wall and of the grouted bars is shown in Fig. C2.

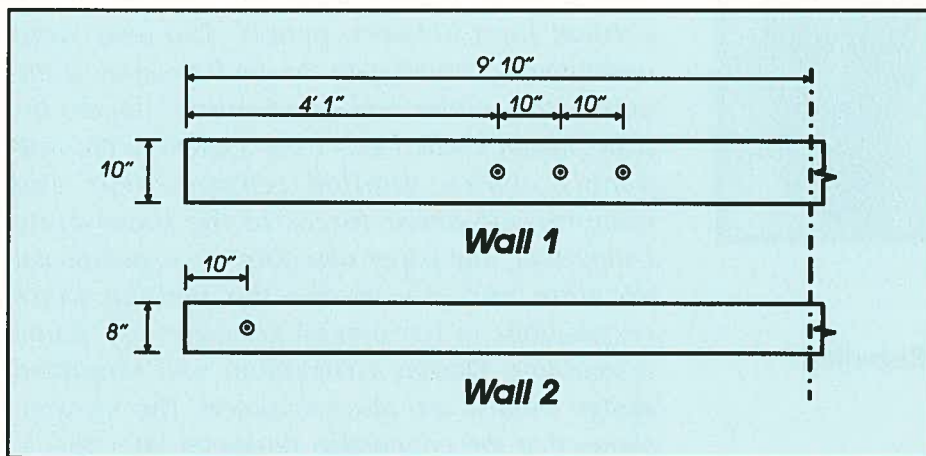


Fig. C2. Location of ducts and connecting bars in Walls 1 and 2.